Journal of Engineering and Applied Science Vol. 4, No. 1, pp. 20–33, June 2020

Journal of Engineering and Applied Science

Contents are available at www.jeas.ruet.ac.bd

Rover End Effector Design for Material Extraction from Earthlike Planets

Md. Rokunuzzaman*, Md. Sabbir Ahmed, Md. Rakibul Islam

Department of Mechanical Engineering, Rajshahi University of Engineering & Technology, Bangaldesh

ARTICLE INFORMATION

Received date: 15 Jan 2020
Revised date: 20 Apr 2020
Accepted date: 07 Jun 2020

Keywords

Earth like planet
End Effector
Mars Rover
Material Extraction
Robotic Gripper

ABSTRACT

In exploration of any earth-like planet, it is very essential to a robot to collect material sample from that planet. Therefore the robot must have some end effector which can extract material from that surface. In this work, by considering various parameters, a scoop type end effector having three degree of freedom has been designed to reduce the resistance force of extraction materials. First the kinematic analysis of the end effector and static torque calculations is analyzed and a prototype has been fabricated with a servo-controlled system. The performance of the end effector has been evaluated by performing several experiments such as extracting soil and burned coal materials. The lowest amount of time during one operation is 21 seconds and maximum weight of the materials extracted has been found as 89 grams. The prototype with proper modifications can also work for extracting ammunitions and underground explosives that are too dangerous for the human being or difficult to handle.

1. Introduction

Robots are sent to explore space without having to worry so much about its safety. Of course, these carefully built robots needed for sticking around to investigate and send information about its destinations. Sending a robot to space is also much cheaper than sending a human. It can survive in space for many years and can be left out there, that means no need for a return trip. Moreover, robots can do lots of things that humans cannot. Some can withstand harsh conditions, like extreme temperatures or high levels of radiation. Robots can also be built to do things that would be too risky or impossible for astronauts. The primary focus on this paper is to develop a novel and simplified design of an end effector of a robotic rover with cheap and locally available materials, so that it can extract material from surface. The motivations behind this work is to cope up with challenged environment and also to increase the flexibility and success in gripping and extracting materials, so that the rover can compete with the exploration challenges.

*Corresponding authors: Department of Mechanical Engineering, Rajshahi University of Engineering & Technology, Bangaldesh
Email address: rzaman@me.ruet.ac.bd (Md. Rokunuzzaman)

2. Review of End Effectors and Research Gap

In robotics, an end effector is the device at the end of a robotic arm, designed to interact with the environment. The end effector means the last link (or end) of the robot. At this endpoint the tools are attached. The exact nature of this device depends on the application of the robot [1]. Most of the literature are associated with Mars rover, which are sent to Mars, as earth like planet. A Mars rover is an automated motor vehicle that propels itself across the surface of the planet Mars upon arrival. Rovers have several advantages over stationary landers: they examine more territory, and they can be directed to interesting features, they can place themselves in sunny positions to weather winter months, and they can advance the knowledge of how to perform very remote robotic vehicle control [2].

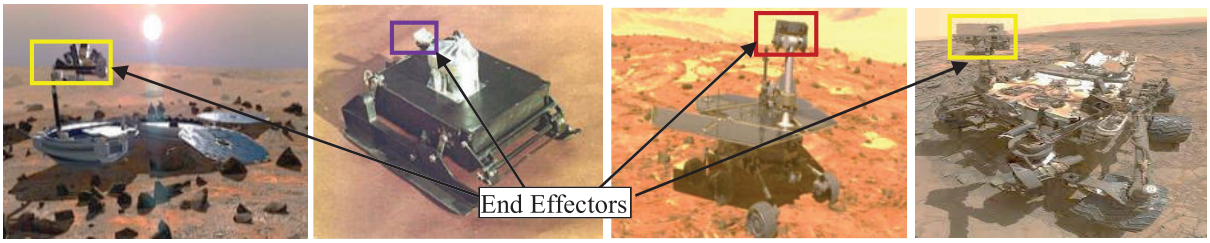

(a) Beagle 2 [3] (b) Mars 3 (Prop-M) [4] (c) Spirit (MER-A) [5] (d) Opportunity (MSL) [6]

Figure 1. Mars Rovers with different types of End Effectors .

NASA sends different types of Rover in MARS surface for exploration of the planet and the rovers are equipped with different types of end effectors. Seven rovers have been dispatched to Mars such as Mars 2 (1971), Mars 3 (1971), Sojourner rover (1997), Beagle 2 (2003), Spirit (MER-A) (2004), Opportunity (MER-B)(2004), Curiosity (2011). Figure 1 shows a few MARS rover missions that has been incorporated till now. Figure 1(a) shows Beagle 2, Planetary Undersurface Tool, lost with Beagle 2 on deployment from Mars Express in 2003. Figure 1(b) shows Mars 3, Prop-M rover that has been sent in 1971, Mars 3 lander has stopped communicating about 20 seconds after landing. Figure 1(c) shows Spirit (MER-A), Mars Exploration rover, has been launched on June 10, 2003 and has landed successfully on January 4, 2004. Figure 1(d) shows Opportunity, Mars Science Laboratory (MSL), by NASA, has been launched November 26, 2003 at and landed in the Aeolis Palus plain near Aeolis Mons (informally "Mount Sharp") in Gale Crater on August 6, 2004.

There are several types of end effector available for Mars rover. Some end effector are drilling type end effector, some are pneumatic type, some are hydraulic type and some are scoop type end effector. Some Mars rover end effector are shown in Figure 2.

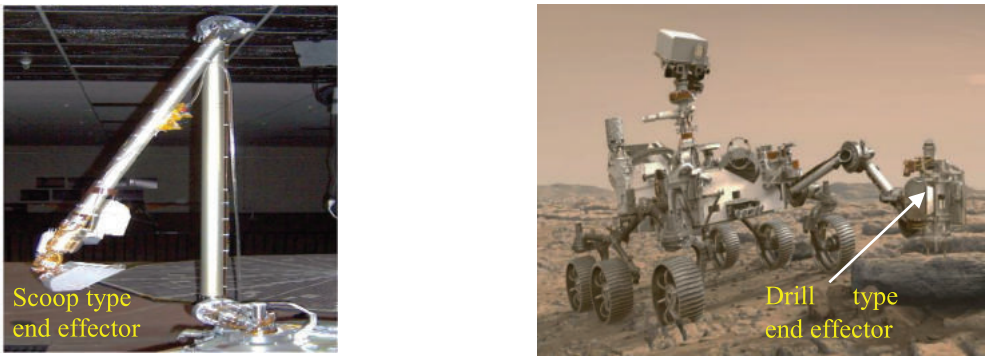

Figure 2. Robotic end effectors for NASA Mars 2007 Phoenix Lander and Curiosity Mars Rover [7].

There are very few literatures relating the rover end effector design available. End effectors for rover can be different types such as parallel 2 finger end effector which can raise up to 5 kg load [8], 3 joints gripper to pick and place of lightweight materials [9]. Tony Jorden et. al designed a sample robotic system for handling samples of material on

planetary surfaces. From the ESA-funded Mars Surface Sample Transfer and Manipulation Study, the authors designed a testing facility with end effector using locking and unlocking mechanism. In this mechanism, they used retractable hex-key for tightening, custom made interchange (Al or Ti) locking jaws, harmonic drives, motors and micro switches [10]. It is very difficult to find the detail designs and data for end effectors specifically for rover. Most of the researches are carried out by NASA and the research methodology, data of the designs are highly confidential. NASA arranges various competition among global university students to find their best throughput. In future, these are utilized in their research. Therefore, this paper is intended to find the detail methodology of the end effector design for earth-like planets. Since, it is not possible to get the data of the Mars surface, this paper compare it with Earth surface with rocky areas where similarity exists. The research gap of this work is stated as:

a) Almost all the Mars rover used complex end effector that consumes more power. There is no simple end effector for energy saving of Mar rover.
b) There is no design model of double scoop that can extract and also grip materials.
c) Shape optimization for economic structure of end effector design was not investigated.
d) No specific study on design of end effectors of Mars rover.
e) No specific kinematic analysis of Mars rover end effector.

Therefore, the objective of this research is to design a simple, economic end effector for material extraction which can be used in rover similar to Martian surface.

3. Design Methodology

System Overview

An overview of the system is given below in Figure 3.

The first step is the search and analysis of information from various sources in accordance with the classic methodology of investigation. Depending on this information the first geometric model has been made which is necessary to make the models of the end effector. A geometric model has been designed with CAD software for mechanical and control system. For mechanical design, Solid Works software and the control system is designed with Proteus [11]. After the CAD design mechatronics integration has been worked out. This integration creates a virtual model that allows to modify the design variables with an ease. The design modifications of the end effector can be easily done from the disciplines of the mechatronic, evaluating its influence and acting. By finishing the design stage, the fabrication of the prototype has been carried out.

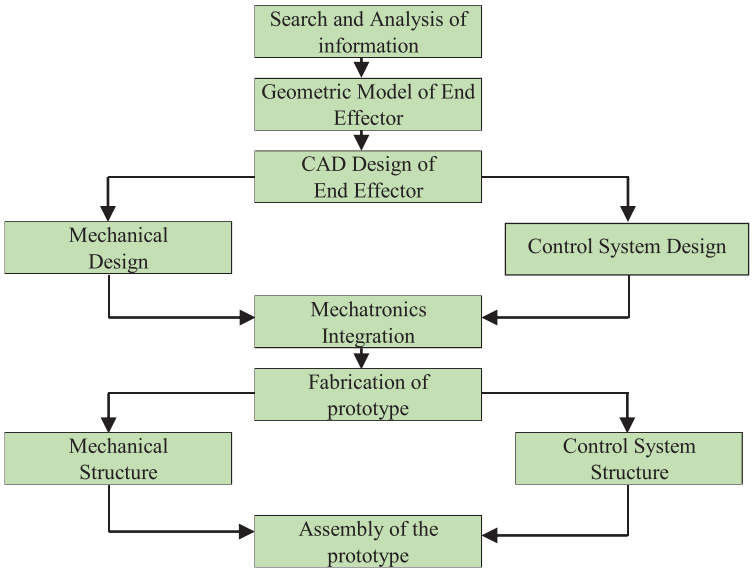

Figure 3. System overview of prototype end effector .

The fabrication of prototype includes two types of fabrications, they are: mechanical and electronics. After finishing the fabrication, the final assembly of the prototype has been done.

Mechanical Design of the End Effector

The mechanical design of the end effector is based on the following design considerations:

(a) The size and shape of the end effector is considered small because of its material cost and motor load capacity.
(b) Simple physical structure as limitations in cost.

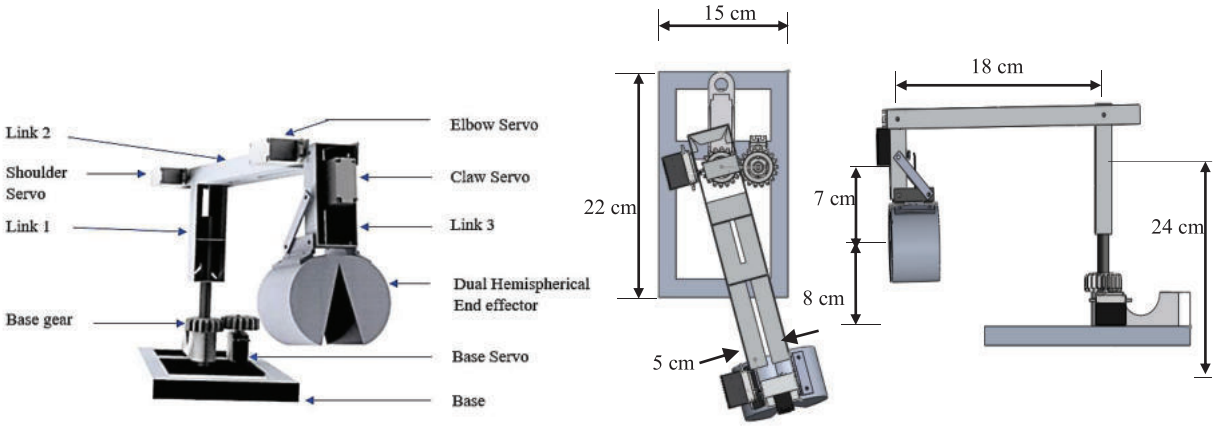

Figure 4. CAD Design of Prototype End Effector .

The prototype is designed using SolidWorks software. Figure 4 shows the CAD design of the end effector. In this work 4 servo motors (Servo Motor MG995) are used (Base Servo, Shoulder Servo, Elbow Servo and Claw Servo) for the total completion of the movement. The dual hemispherical end effector is operated by the link and claw servo. The purpose of using servo motors is to determine the position of the shaft and control the position very precisely. The purpose of using 4 servo motors is to obtain 4 degrees of freedom position of the end effector and also to get different movements of the end effector, so that it can be operated precisely and smoothly. Microcontroller (Atmega328) is used to control the whole system due to its more PWM pin and low cost. Command is sent to the controller and the controller controls the servo to operate precisely so that it can extract material via the end effector. A wired communication system like joystick is used to communicate with the microcontroller. Joystick is used as a simple medium of communication to operate the end effector manually.

Possible Design Alternatives and Selection of End Effector

Table 1. Comparison of possible end effector .

Requirements	Shovel	Drill	Hand
Resistance force	B	B	B
Number of actuators	A	B	C
Durability	A	C	C
Scooping ability	A	B	C
Digging ability	A	A	C

Here,

"A" indicates that the shape adequately fulfills the corresponding requirements.

"B" indicates that the shape may modestly manage the requirements.

Table 2. End effector type selection.

Shovel	Drill	Hand
1. Few actuators and its shape consist of a single part, 2. It can adapt to a variety of samples.	1. Capable of digging deep into the soil 2. Mechanisms are more complicated, which results in low durability.	1.The hand shape requires several mechanical joints and bearings that are indispensable for its dexterity.

To find the best possible design for the end effector, Table 1 and Table 2 is formed based on some assumptions or concepts. From on the comparisons given in Table 1 the shovel shape is selected for material extraction for fulfilling the requirements and given in Table 2.

End Effector Kinematics

The non-rotating reference Frame {0} is attached to a fixed point at the center of the rotary base. Frame {1} corresponding to Link (1) is attached at its upper end. It is to be noted that the origin of this frame could have been appointed to any location along Link (1) since Z_0 and Z_1 are parallel to each other. Frame {2} rotates with Link (2) and is located at the intersection between Link (1) and Link (2), thus having X_2 along the common perpendicular pointing from Z_2 to Z_3. Frame {3} rotates with Link (3) and is attached at its intersection with Link (2). Finally, Frame {4} corresponding to the end-effector is located midway between the two grippers [12].

The kinematics analysis of the system is given below in Figure 5.

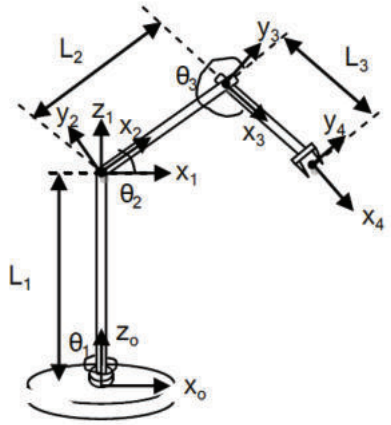

Figure 5. Kinematic Analysis of End Effector.

Based on the defined frames, the Denavit-Hartenberg (D-H) parameters are determined as shown in Table 3.

Table 3: The D-H parameters.

i	α_{i-1}	a_{i-1}	d_i	θ_i
1	0°	0	L_1	θ_1
2	90°	0	0	θ_2
3	0°	L_2	0	θ_3
4	0°	L_3	0	0°

The homogeneous transformation matrices describing the end-effector frame with the reference frame can be formalized by equation 1 as:

$$ {}^{0}_{4}T = \begin{bmatrix} C_1C_{23} & -C_1S_{23} & S_1 & C_1C_{23}L_3 + C_1C_2L_2 \\ S_1C_{23} & -S_1S_{23} & -C_1 & S_1C_{23}L_3 + S_1C_2L_2 \\ S_{23} & C_{23} & 0 & S_{23}L_3 + S_2L_2 + L_1 \\ 0 & 0 & 0 & 1 \end{bmatrix} \quad (1) $$

The first three entries of the last column in ${}^{0}_{4}T$ represent the Cartesian coordinates of the position of the origin of the end effector frame {4} with respect to the reference frame {0}.

$$ X = C_1C_{23}L_3 + C_1C_2L_2 \quad (2) $$

$$ Y = S_1C_{23}L_3 + S_1C_2L_2 \quad (3) $$

$$ Z = S_{23}L_3 + S_2L_2 + L_1 \quad (4) $$

Here, C_{23} is the cosine of the sum of θ_2 and θ_3 [$\cos(\theta_2+\theta_3) = C_{23}$] and S_{23} is the sine of the sum of these two angles [$\sin(\theta_2 + \theta_3) = S_{23}$].

And $\Phi = \theta_1 + \theta_2 + \theta_3$

The procedure for obtaining the analytical expression for the x, y and z coordinates is called forward kinematics analysis [13][14]. The forward kinematics, Equation 2 to 4, produce the position of the end effector as a function of the joint anglesθ_1, θ_2 and θ_3.

In the inverse kinematics, the position coordinates equations, Equation 2 - 4, has been used to find the analytical expressions of the rotational angles (i.e.θ_1, θ_2 and θ_3) for the waist, shoulder and elbow motors as a function of the desired *x*, *y* and *z* coordinates. The derivation of the inverse kinematic equations is summarized as follows:

Firstly, dividing Eq. 3 by Eq. 2 gives,

$$ \frac{Y}{X} = \frac{S_1C_{23}L_3 + S_1C_2L_2}{C_1C_{23}L_3 + C_1C_2L_2} = \frac{S_1(C_{23}L_3 + C_2L_2)}{C_1(C_{23}L_3 + C_2L_2)} = \frac{S_1}{C_1} = \tan\theta_1 \quad (5) $$

As a result, θ_1 is explicitly expressed as,

$$ \theta_1 = \text{atan2}\left(\frac{Y}{X}\right) \quad (6) $$

The (atan2) function generates the arctangent of the argument and the proper quadrant based on the signs of both the denominator and the numerator.

Furthermore, by summing up the squares of Equation 2 to 4 and rearranging one can obtain an explicit expression for the cosine of θ_3 as a function of the robotic arm geometry and the coordinates of the target point.

$$ C_3 = \frac{X^2 + Y^2 + Z^2 - \left(L_1^2 + L_2^2 + L_3^2\right) - 2L_1(Z - L_1)}{2L_2L_3} \quad (7) $$

From the Pythagorean trigonometric identity,

$$S_3 = \pm\sqrt{1 - C_3} \tag{8}$$

It should be noted that the ambiguity in algebraic sign in the above equation, Eq. 8, is an indication of multiple solutions. The two solutions correspond to the two different configurations that the arm could take to reach the same point (i.e. elbow up and elbow down). Accordingly, from the previous,

$$\theta_3 = \text{atan2}\left(\frac{S_3}{C_3}\right) \tag{9}$$

Considering Eq. 4, applying the angle addition trigonometric identity, and defining the following variables,

$$K_1 = (C_3L_3 + L_2) \qquad K_2 = (S_3C_3)$$

It can be shown that,

$$Z - L_1 = (K_1S_2 + K_2C_2) \tag{10}$$

$$(Z - L_1)^2 = (K_1S_2 + K_2C_2)^2 \tag{11}$$

Then by expanding the left side and regrouping the terms, the following quadratic equation can be obtained,

$$(K_1^2 + K_2^2)S_2^2 + 2K_1(L_1 - Z)S_2 + (Z^2 + L_1^2 - K_2^2 - 2ZL_1) = 0 \tag{12}$$

Using the quadratic formula, θ_2 can be expressed in terms of the robotic arm geometry, the target point z- coordinate, and the value of θ_2 as obtained from Eq. 9,

$$\theta_2 = \sin^{-1}\left(\frac{A \pm\sqrt{B}}{2(K_1^2 + K_2^2)}\right) \tag{13}$$

Where,

$$A = -2K_1(L_1 - Z) \qquad B = [2K_1(L_1 - Z)]^2 - 4(K_1^2 + K_2^2)(Z^2 + L_1^2 - K_2^2 - 2ZL_1)$$

It can be noticed from Eq. 13 that there are two solutions, roots, for θ_2. It is noteworthy that there is another approach to find θ_2. To obtain this alternative formula for θ_2, the *x* and *y* coordinates equations, Eqs. 2 and 3, should be rewritten as

$$X = C_1(K_1C_2 - K_2S_2) \tag{14}$$

$$Y = S_1(K_1C_2 - K_2S_2) \tag{15}$$

In obtaining Eq. 14 and 15, the trigonometric angle addition identity was used. Now by subtracting Eq. 15 from Eq. 14,

$$\frac{X-Y}{C_1-S_1} = K_1C_2 - K_2S_2 \quad (16)$$

Together with Eq. 10, Eq. 16 constitute a system of two transcendental equations that can be solved by transformation to polar coordinates using,

$r = \sqrt{(K_1)^2 + (K_2)^2}$ And $\gamma = atan2\left(\frac{K_2}{K_1}\right)$ to give

$K_1 = r\cos\gamma$ and $K_2 = r\sin\gamma$ thus,

$$\frac{X-Y}{C_1-S_1} = rC_\gamma C_2 - rS_\gamma S_2 \quad (17)$$

Applying the angle addition trigonometric identity,

$$\frac{X-Y}{r(C_1-S_1)} = \cos(\gamma+\theta_2) \quad (18)$$

From Eq. 10, using the same transformation and the angle addition trigonometric identity, can be written as

$$\frac{Z-L_1}{r} = \sin(\gamma+\theta_2) \quad (19)$$

Dividing Eq. 19 by Eq. 18 and substituting for the values of K_1, K_2, r and γ,

$$\theta_2 = atan2\left[\frac{(Z-L_1)(C_1-S_1)}{(X-Y)}\right] - atan2\left[\frac{S_3L_3}{(C_3L_3+L_2)}\right] \quad (20)$$

Equation 20 offers another way to explicitly compute θ_2. However, both methods are supposed to produce the same result. Therefore, just by substituting the target x, y and z coordinates into Eqs. 6, 9, and 13 (or 20) will generate θ_1, θ_2 and θ_3, after which the robotic arm links will rotate accordingly to reach that location in space.

Elbow angle, $\theta_3 = \Phi - \theta_1 - \theta_2$

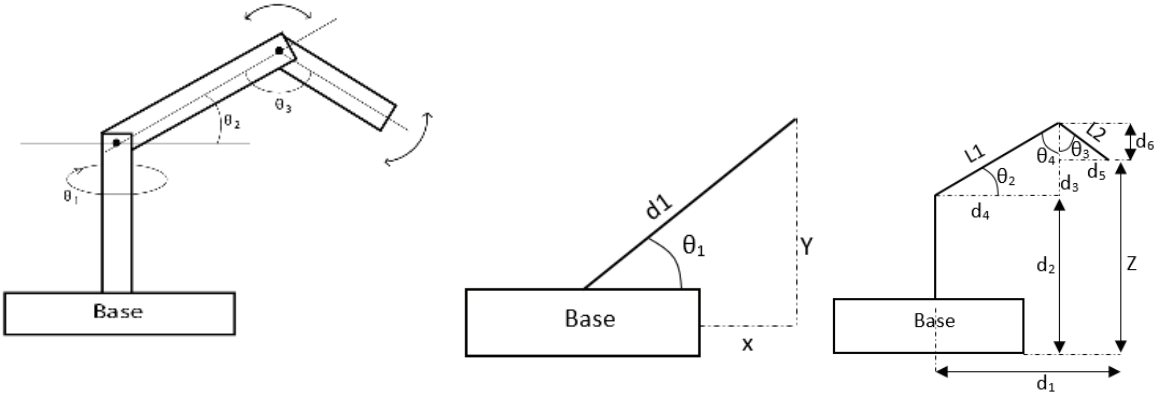

Figure 6. Position calculation of the end effector.

Figure 6 shows the position calculation of the end effector where, L_1 is the Shoulder length of the robot and L_2 is the elbow length, θ_1 is the base rotating angle of robot where θ_2 and θ_3 are the shoulder and elbow rotating angles respectively. According to Figure 4, L_1 = 18 cm, θ_1 = 60°, L_2 = 16.9 cm, θ_2 = 30°, d_2 = 22 cm, θ_3 = 130°

The angles are determined from the figures,

θ_4 = 180° - 30° - 90° = 60°

$\theta_5 = \theta_3 - \theta_4$ = 130° - 60° = 70° and position of the end effector tip (*X, Y, Z*) can be calculated as

$X = d_1 cos\theta_1$ =15.735 cm

$Y = d_1 sin\theta_1$ =27.25 cm

$Z = d_2 + L_1 sin\theta_2 - L_2 cos\theta_5$ =25.22 cm

Static Torque of the End Effector

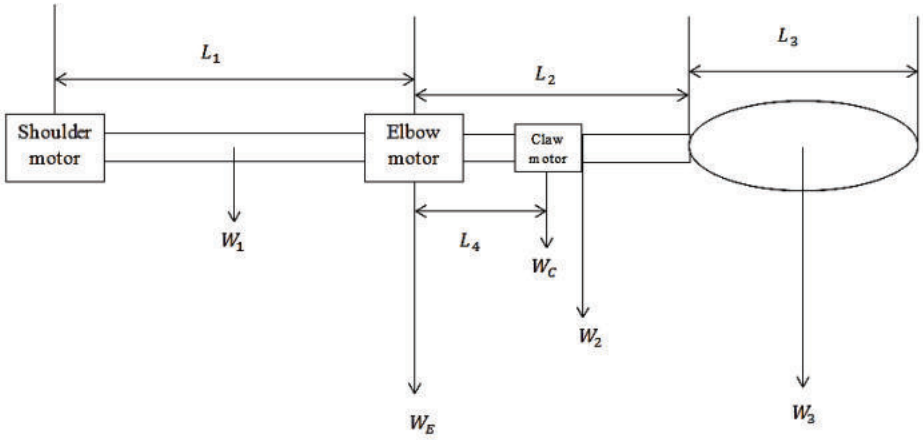

Figure 7: Free body diagram of the robotic arm .

W_1= Weight of link 1 = 80g

W_2= Weight of link 2 = 30g

W_3= Weight of link 3 = [Weight of end effector (100g) + Weight of extracted material (150g)]

W_C= Weight of claw motor = 50g, W_E= Weight of elbow motor = 50g, L_1= 18 cm, L_2= 7 cm, L_3= 8 cm, L_4= 3 cm

Equations for calculating the required torque are given below according to the Figure 7.

$$T_{Elbow} = (W_C \times L_4) + \left(\frac{1}{2} \times L_2 \times W_2\right) + \left[W_3\left(L_2 + \frac{1}{2}L_3\right)\right]$$

$$= (50 \times 3) + \left(\frac{1}{2} \times 7 \times 30\right) + \left[250\left(7 + \frac{1}{2} \times 8\right)\right] = 3.005 \text{ kg-cm}$$

$$T_{Shoulder}=\left(W_1 \times \frac{1}{2}L_1\right) + (W_E \times L_1) + [W_C(L_1 + L_4)] + \left[W_2\left(L_1 + \frac{1}{2}L_2\right)\right] + \left[W_3\left(L_1 + L_2 + \frac{1}{2}L_3\right)\right] = \left(80 \times \frac{1}{2} \times 18\right) + (50 \times 18) + [50(18+3)] + \left[30\left(18 + \frac{1}{2} \times 7\right)\right] + \left[250\left(18 + 7 + \frac{1}{2} \times 8\right)\right]$$

= 10.565 kg-cm

From the moments equilibrium equations which are shown above, the results minimum torque of elbow and shoulder motor are 3.005 kg-cm and 10.565 kg-cm respectively.

Final minimum torque needed of joints of robot after considering the safety factor (1.5) is given below-

T_{Elbow}= 1.5×3.005 = 4.5075 kg-cm (Approximately)

$T_{Shoulder}$= 1.5×10.565 = 15.8 kg-cm (Approximately)

Since the value of $T_{Shoulder}$ is big enough that locally available servo cannot sustain at this torque. Therefore, a spring is added between the link 1 and link 2.

Control system Design

The end effector is controlled by a microcontroller ATMEGA 328P and a joystick. The PCB with various electronic components are designed with Proteus software. The complete circuit diagram is shown in Figure 8.

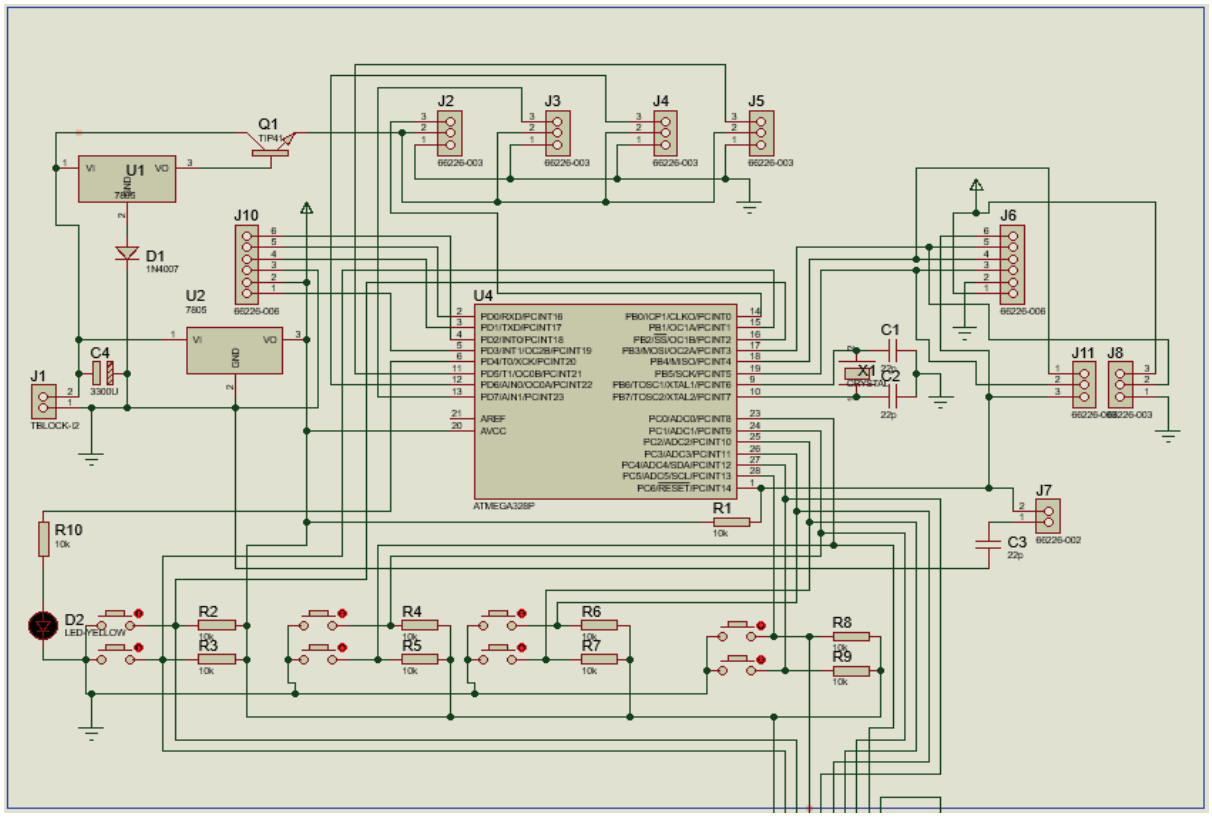

Figure 8: Complete circuit diagram of end effector control.

4. Fabrication and Assembly of End Effector

After the mechatronics integration of mechanical design and control system design, the fabrication process of end effector prototype has been carried out by manually in the machine shop of RUET. The parts needed for fabrication has been found partly in the machine shops and others were bought from local market. Various manufacturing operations such as cutting, drilling, joining etc. are required to fabricate and assemble the designed prototype. Figure 9 shows different fabricated mechanical structures such as base, bearing mounting on base, link1 and shoulder joint, link2 and elbow joint, link 3 and scoop at the last in the figure.

Fabrication of Mechanical Structure

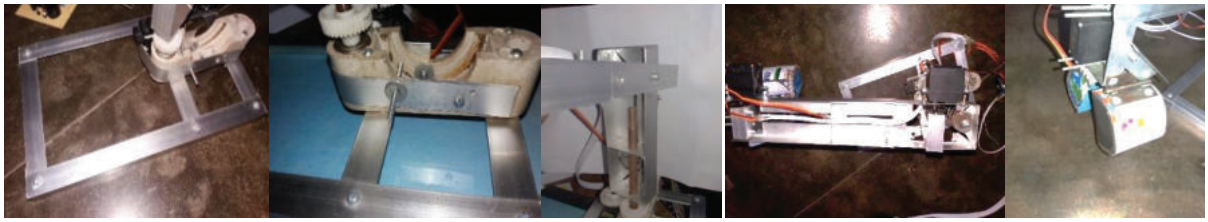

Figure 9: Photographs of fabricated Mechanical structures for end effector.

Fabrication of Control Structure and Final Assembly

Figure 10 shows the assembled electronic components on a PCB and a control joystick fabricated with Veroboard and push buttons. Connection has been made by jumper wires with the microcontroller PCB. The final assembly is shown at the end of this figure.

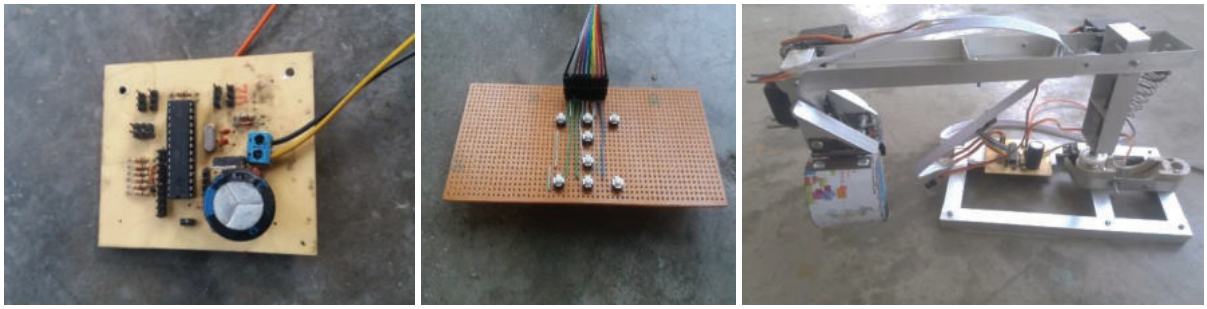

Figure 10: Photographs of fabricated control structures and final assembly.

5. Experimental Results

For experiment, the robot end effector is placed in outdoor environment from where it can extract material. The Experimental Setup is shown in the Figure 11. In this setup, two boxes, one box from which material has been extracted and another box in which material is unloaded. The time for loading and unloading has been calculated and the total time from the initial position after doing work return to the neutral position is calculated. For the experiment two types of experimental material, one is soil and other is burned coal is used.

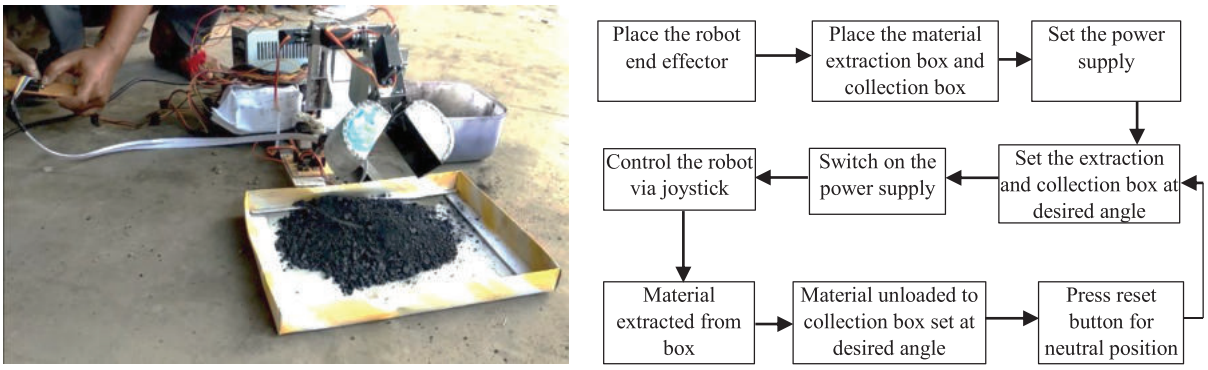

Figure 11: Experimental setup and Testing Procedure .

Results for extraction of sample soil materials

In figure 12 the end effector has extracted soil materials of various quantities and places the materials at desired position. The experiment has been performed to place the materials at 45°, 90° and 120° angles with respect to box positions.

Similar experiments are done for burned coal materials of various quantities and places the materials at desired position and are shown in figure 13.

After extracting materials, the weight of sample materials per case are measured with a digital weight balance. Result of the experiments are given in table 4 and table 5.

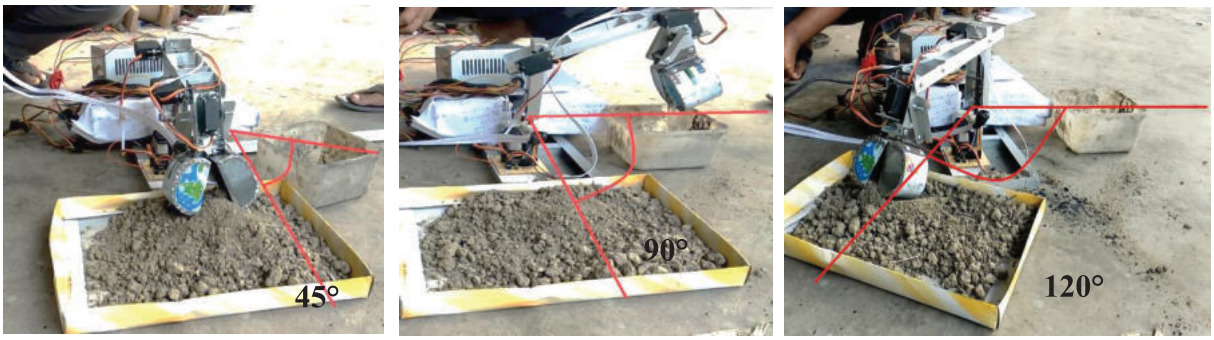

Figure 12: Extraction of soil samples at various positions .

Figure 13: Extraction of burned coal samples at various positions .

Table 4: Data for extracting soil material from surface.

Material	Angle (Degree)	Time of loading (Second)	Time needed to change the position of end effector (Second)	Time of unloading (Second)	Total time between loading and unloading (Second)	Error in Average Value (Second)	Weight of extracting material (Gram)
Splits of soil	45°	12	4	5	21	±1	69
		11	5	6	22		81
		12	5	5	22		67
	90°	11	6	6	23	±2.5	89
		12	8	8	28		70
		11	7	8	26		67
	120°	14	10	7	31	±1.5	71
		13	9	6	28		68
		12	10	8	30		71

From the experimental data of Table 4 and Table 5, the abilities and performance of the end effector are summarized as:

(a) Minimum and maximum time of loading of end effector for both the materials are 11 seconds and 14 seconds respectively.
(b) Minimum and maximum time of unloading of end effector for both the materials are 5 seconds and 9 seconds respectively.
(c) Minimum and maximum time to change the position of end effector for both the materials at 45° angle are 4 second and 5 seconds, at 90° angle are 6 seconds and 8 seconds and at 120° angle are 9 seconds and 10 seconds respectively.
(d) Minimum and maximum total time between loading and unloading for both the materials at 45° angle are 21 seconds and 28 seconds, at 90° angle are 23 seconds and 29 seconds and at 120° angle are 28 seconds and 31 seconds respectively.

Maximum weight that can be extracted by the end effector is 89 gm. In compared to a similar end effector designed in [15], the maximum weight carried is less than 50 gm. Therefore, this end effector is better by weight lifting.

Table 5: Data for extracting burned coal from surface.

Material	Angle (Degree)	Time of loading (Second)	Time needed to change the position of end effector (Second)	Time of unloading (Second)	Total time between loading and unloading (Second)	Error in Average Value (Second)	Weight of extracting material (Gram)
Splits of burned coal	45°	14	5	9	28	±2	62
		12	4	7	23		51
		13	4	8	25		64
	90°	12	8	7	27	±1	60
		14	6	8	28		55
		13	7	9	29		59
	120°	11	10	8	29	±1	56
		14	9	7	30		47
		13	10	8	31		63

Loading and unloading time depends on two factors: traversing distance and speed of operation. Moreover, traversing distance depends on angle and speed of operation depends on motor speed controlled by Joystick. Since the end

effector is operated manually, it is not possible to maintain same speed all the instant. That's why loading and unloading time varies with angle.

6. Conclusion

After examining the requirements, the most appropriate shovel type end effector has been selected and proposed to reduce resistance force. An end effector for material extraction from earth like surface has been successfully designed and fabricated using cheap and locally available materials. The fabricated model of the robot has been also provided with correct joint angles to move end effector to required position and orientation within its workspace. The prototype has been experimented with two types of materials, one is splits of soil and another is splits of burned coal. The average time needed from extracting to unloading the materials from both material surface for 45° is 23.5 seconds, for 90° is 26.83 seconds and for 120° is 29.83 seconds. The weight of material extracted from soil surface is 72.55 gm and from burned coal surface is 57.44 gm. The performance of the robotic end effector for material extracting from a surface closely to Mars is quite satisfactory. However, the performance of the system could be exalted further to produce more accurate and reliable results. Some of the recommendations for such improvement include increasing the ability of digging the surface to extract material from hard rocky surface by using hydraulic system or linear actuator, design and implementation of different types embedded sensors to achieve vibration control and smooth motion of end effectors, wireless control of the robotic end effector. The scopes of this type of end effectors are: in the applications of extracting the ammunition that is undergrounded due to dangerous to human being, extracting or removing something from surface where human being can't reach, picking and placing the materials from inconvenient environment, raising the explosives that is hidden in any place, applying for industrial purpose where human being can't perform the job.

7. References

[1] Gareth, M. J., Robot grippers, Wiley-VCH, pp.20-22, 2007.
[2] J. P. Grotzinger, D.Y. Sumner et al, "A habitable fluvio-lacustrine environment at Yellowknife Bay, Gale crater, Mars", Journal of Science (New York, N.Y.), Vol. No. 343, pp.127-153, January, 2014.
[3] Davis N. Beagle 2: most detailed images yet of lost Mars lander revealed, Article, The Gaurdian, 2016, accessed in 21 January 2019 from https://www.theguardian.com/science/2016/apr/26/beagle-2-most-detailed-images-yet-of-lost-mars-lander-revealed.
[4] Is there any chance Mars-3's Prop-M rover deployed automatically, Article, Space Exploration Stack Exchange. Stack Exch 2017, accessed in 3 December 2018 from https://space.stackexchange.com/questions/21709/is-there-any-chance-mars-3s-prop-m-rover-deployed-automatically-and-roved.
[5] G. Curt, Our Spaceflight Heritage: Mars Exploration Rover Spirit remembered 13 years after landing, Space Flight Insider, 2017, accessed in 3 December 2018 from https://www.spaceflightinsider.com/space-flight-history/spaceflight-heritage-13-year-anniversary-mars-rover-spirit-landing.
[6] Five things about NASA's Mars Curiosity rover, Article, accessed in 5 February 2019 from https://www.nasa.gov/mission_pages/msl/msl5things20100916.html.
[7] B, R. Carsten and L. O Shiraishi, "The Phoenix Mars Lander Robotic Arm", IEEE Aerospace conf., Vol.No.1, pp.1-12, 2009.
[8] R. Bonitz, J. Slostad, B. Bon, D. Braun, R. Brill and C. Buck, "Mars Volatiles and Climate Surveyor Robotic Arm", Journal of Geophysical Research E: Planets, Vol. No.106(E8), pp.17623-34, 2001.
[9] M. Farman, M. Al-shaibah, Z. Aoraiath and F. Jarrar, "Design of a Three Degrees of Freedom Robotic Arm", International Journal of Computer Applications, Vol. No. 179, pp.12-17, 2018.
[10] T. Jorden, E. Allouis et al, "Testing a Robotic System for collecting and transferring samples on Mars", research paper, Astrium Ltd, Gunnels Wood Road, Stevenage, SG1 2AS, UK, 2018.
[11] J. Shah, K. Nit et al, "End Effector Position Analysis Using Forward Kinematics For 5 DOF Pravak Robot Arm", IAES International Journal of Robotics and Automation (IJRA), Vol. No. 2, pp.112-116, 2013.
[12] B. Fernini, K. Brahim, "Kinematic Modeling and Simulation of a 2-R Robot by Using Solid Works and Verification by MATLAB / Simulink", European Journal of Scientific Research, Vol.No.1, pp.78-93, 2012.
[13] T. P. Singh, P. Suresh, and S. Chandan, "Forward and Inverse Kinematic Analysis of Robotic Manipulators", International Research Journal of Engineering and Technology (IRJET), Vol. No. 4, Issue.2, February, 2017.
[14] J. J. Craig, Introduction to Robotics: Mechanics and Control, Pearson, 3rd edition, pp. 101-134, 2005.
[15] A. Elfasakhany, E. Yanez, K. Baylon and R. Salgado, "Design and Development of a Competitive Low-Cost Robot Arm with Four Degrees of Freedom", Modern Mechanical Engineering, Vol. No.1, pp. 47-55, 2011.